

## References

- 1 YAMADA, M., SAITOH, M., and OOKI, H.: 'Electric-field-induced cylindrical lens; switching and deflection devices composed of the inverted domains in LiNbO<sub>3</sub> crystals', *Appl. Phys. Lett.*, 1996, **69**, pp. 3659–3661
- 2 GAHAGAN, K.T., GOPALAN, V., ROBINSON, J.M., JIA, Q.X., MITCHELL, T.E., KAWAS, M.J., SCHLESINGER, T.E., and STANCIL, D.D.: 'Integrated electro-optic lens/scanner in a LiTaO<sub>3</sub> single crystal', *Appl. Opt.*, 1999, **38**, pp. 1186–1190
- 3 WEIS, R.S., and GAYLORD, T.K.: 'Lithium niobate: summary of physical properties and crystal structure', *Appl. Phys. A*, 1985, **37**, pp. 191–203

## Very low crosstalk 1×2 digital optical switch integrated with variable optical attenuators

M.-S. Yang, Y.O. Noh, Y.H. Won and W.-Y. Hwang

A novel digital thermo-optic switch based on a polymer waveguide has been demonstrated. The proposed switch consists of a conventional 1×2 digital optical switch and compact variable optical attenuators, with both elements integrated in series. The switches exhibit very low crosstalk values of  $-42$  and  $-40$  dB, and the switching power is  $\sim 170$  mW at  $1.55\mu\text{m}$ .

**Introduction:** Polymeric thermo-optic (TO) waveguide devices have received great attention due to their superior characteristics such as low power consumption and ease of fabrication, etc. Optical switches are key elements in the construction of all-optical transmission and switching networks [1]. Such switches have been realised in a variety of device structures. Among these, digital optical switches (DOSs) based on adiabatic mode evolution benefit greatly from their digital response, which gives polarisation-independent switching characteristics, low crosstalk, stable switching characteristics, etc. [2]. To obtain low switching crosstalk in a conventional DOS, the branch angle is normally designed to range from  $0.05$  to  $0.12^\circ$ . However, the small Y-branch angle causes many difficult problems in the fabrication process, with the result that crosstalk is usually worse than expected. Many authors have reported wide-angle DOSs that are easy to fabricate and achieve a low switching power without adversely affecting the crosstalk [3–5].

In this Letter, we propose a new switch structure in which variable optical attenuators (VOAs) are integrated with a conventional 1×2 DOS in series. The integration of the compact VOAs gives highly improved crosstalk characteristics compared with those of a conventional 1×2 DOS. In addition, the Y-branch angle can be increased without affecting the crosstalk. Therefore the overall switching power including the VOAs is not significantly increased because the electrode length of the DOS can be shortened if the Y-branch angle becomes wide.

**Operation principle:** Fig. 1 shows a schematic diagram of the proposed device, with the variable optical attenuators connected to the end of the Y-branch of a conventional 1×2 DOS. The linear Y-branch has a branching angle of  $\alpha$ . The operation principle of the 1×2 DOS is based on the adiabatic mode evolution and thermo-optic (TO) effect of the polymer waveguide. If electric power is applied to one of the electrodes, the refractive index decreases so that the optical signal is directed to the other arm. This situation is represented by the 'off-state' in the power-applied electrode arm and 'on-state' in the other arm. The residual optical power in the off-state arm is further reduced by applying heat to the VOA connected in the off-state arm, thus enhancing the crosstalk of the device. The crosstalk in the wide-angle DOS itself in Fig. 1 is designed to be lower than  $-20$  dB in this work so that the insertion loss is not affected by the attenuator.

The operating principle of the attenuator is as follows. The device consists of input and output singlemode waveguides, tapering regions, a multimode supporting waveguide region, and electrodes at an angle of  $\beta$ . At first, light is expanded adiabatically into the multimode supporting waveguide region following the Y-branch. When electrical power is applied along the electrode, the refractive index under the heated electrode is lowered by the TO

effect. Therefore, the propagating light is partially reflected at an angle of  $2\beta$  with respect to the propagating direction. If the angle is larger than the fundamental mode of the multimode supporting region, then the reflected light is coupled back into the higher-order modes after passing the heated electrode. These higher-order modes are successively filtered out through the output tapering region and the output singlemode waveguide. As the applied power increases, so too does the amount of reflected light, which then leads to larger attenuation. Details of the attenuator will be published elsewhere [6].

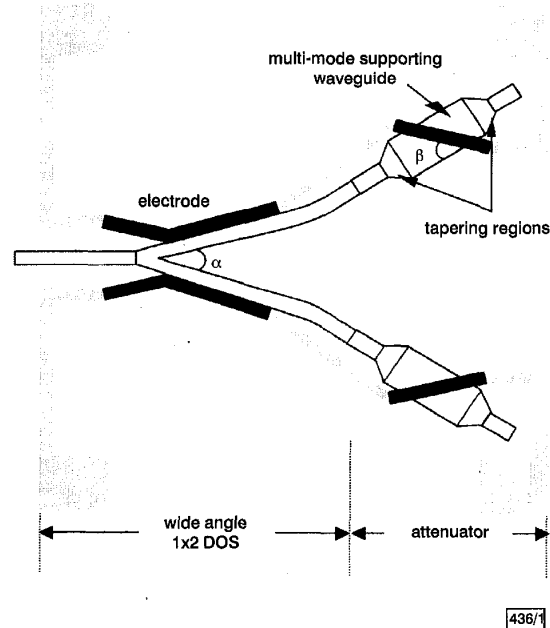


Fig. 1 Structure of proposed wide angle 1×2 digital optical switch

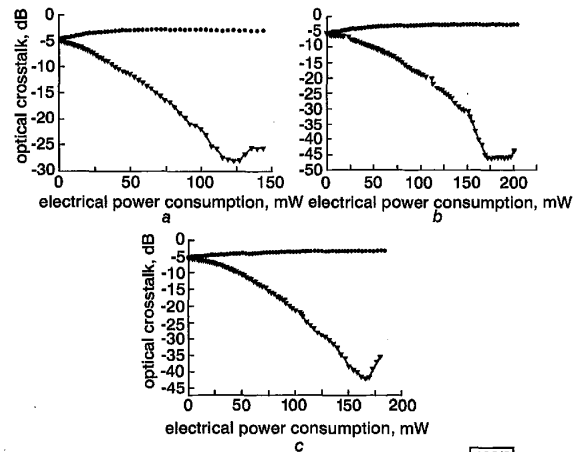


Fig. 2 Measured device characteristics

- a Type (i); conventional DOS with  $\alpha = 0.11^\circ$   
 b Type (ii); proposed switch with  $\alpha = 0.16^\circ$   
 c Type (iii); proposed switch with  $\alpha = 0.25^\circ$  at  $1.55\mu\text{m}$

**Experiment:** The switch was a buried channel type waveguide with a  $7 \times 7 \mu\text{m}^2$  rectangular cross-section. The core and cladding materials were ZP1010™ and ZP2145™, respectively, which were thermally cross-linkable polymers synthesised at ZenPhotonics Co. Ltd. The refractive index difference of the core and the cladding was  $0.7\%$ . The birefringence between the TE and TM modes was  $\sim 0.0036$  at  $1.55\mu\text{m}$  for both the core and cladding.

Three types of switch were designed and fabricated to compare the conventional DOS with ours: type (i) a conventional DOS with  $\alpha = 0.11^\circ$ ; type (ii) the proposed switch with  $\alpha = 0.16^\circ$ ; type (iii) the proposed switch with  $\alpha = 0.25^\circ$ . The electrode width of the DOS and the attenuators was  $7.2\mu\text{m}$  in both cases. In the

attenuators, the width of the multimode supporting region and the electrode angle were 40µm and 1.6°, respectively, and they were optimised to give the minimum power consumption at an attenuation level of 25–30dB.

Figs. 2a, b and c show the measured switching characteristics at 1.55µm. The crosstalk values between the on-state and off-state were –26, –42 and –40dB for types (i), (ii) and (iii), respectively. It can be seen that the crosstalk is greatly enhanced to –42dB in the proposed devices, while the switching powers are 1.5 times larger than for the conventional 1×2 DOS. Figs. 2b and c show the comparison in the crosstalk and switching characteristics of the proposed device according to the Y-branch angles. The effect of the Y-branch angle in the proposed devices is not critical to the switching power and crosstalk except for off-state switching. The flat region and the sharp valley appear in the off-states in types (ii) and (iii). This is because the minimum point in the crosstalk characteristics of the 1×2 DOS as a function of the applied power usually does not coincide with the minimum point in the attenuators. When the two minimum points coincide, the crosstalk curve shows a sharp valley as in Fig. 2c. If they have some offset value between the minimum points according to the applied power, it will show a flat region as in Fig. 2b.

**Conclusions:** We have demonstrated novel 1×2 switches based on polymer waveguides, which consist of a conventional 1×2 DOS and VOAs. The fabricated switches show very low crosstalk values of –42dB at an electrical power consumption of 165–180mW. The fibre-to-fibre insertion loss is below –3.5dB.

© IEE 2001  
Electronics Letters Online No: 20010394  
DOI: 10.1049/el:20010394

22 November 2000

M.-S. Yang, Y.O. Noh and Y.H. Won (Information and Communications University (ICU), PO Box 77, Yusong, Taejon, 305-600, Korea)

E-mail: misung@icu.ac.kr

W.-Y. Hwang (ZenPhotonics Co. Ltd, 104-11, Moonji-Dong, Yusong, Taejon, 305-380, Korea)

## References

- 1 YAO, S., MUKHERJEE, B., and DIXIT, S.: 'Advances in photonic packet switching: an overview', *IEEE Commun. Mag.*, 2000, **38**, (2), pp. 84–94
- 2 VINCHANT, J.F., RENAUD, M., ERMAN, M., PEYRE, J.L., JARRY, P., and PDGNOD-ROSSIAUX, P.: 'Inp digital optical switch: key element for guided-wave photonic switching', *IEE Proc. J*, 1993, **140**, (5), pp. 301–307
- 3 LIU, Y.L., LIU, E.K., ZHANG, S.L., LI, G.Z., and LUO, J.S.: 'Silicon 1×2 digital optical switch using plasma dispersion', *Electron. Lett.*, 1994, **30**, (2), pp. 130–131
- 4 NELSON, W.H., MASUM CHOUDHURY, A.N.M., ABDALLA, M., BRYANT, R., MELAND, E., and NILAND, W.: 'Wavelength- and polarization-independent large angle InP/InGaAsP digital optical switches with extinction ratios exceeding 20dB', *IEEE Photonics Technol. Lett.*, 1994, **6**, (11), pp. 1332–1334
- 5 SIEBEL, U., HAUFFE, R., and PETERMANN, K.: 'Crosstalk-enhanced polymer digital optical switch based on a W-shape', *IEEE Photonics Technol. Lett.*, 2000, **12**, (1), pp. 2000–2001
- 6 NOH, Y.O., YANG, M.-S., WON, Y.H., and HWANG, W.-Y.: 'Novel PLC-type variable optical attenuator operated at low electrical power', *Electron. Lett.*, 2000, **36**, (24), pp. 2032–2033

## Channel estimation method with interference reduction for high-rate personal area networks

Y.-H. You, C.-H. Park, M.-C. Ju, J.-H. Paik, K.-W. Kwon and J.-W. Cho

A channel estimation technique with interference cancellation in a wireless personal area network system with complementary code keying signalling is described. The performance of the proposed coherent detector is compared with that of a non-coherent detector, and a significant performance improvement as a result of the self-interference cancellation feature is observed.

**Introduction:** In recent years, much attention has focused on higher data-rate versions of wireless personal area networks (WPANs), such as the Bluetooth, shared wireless access protocol (SWAP) and wireless local area network (WLAN) protocols [1, 2]. To this end, both the Bluetooth SIG and IEEE 802.15 committee are working towards realising a high-rate version, as well as reducing interference with other wireless communication systems, such as the IEEE 802.11b version, which employs complementary code keying (CCK) for a high-rate waveform [2]. These CCK codes perform well when used with a RAKE receiver in an indoor multipath environment. However, it can be efficiently demodulated assuming accurate knowledge of the multipath channel [3].

In this Letter, we present a simple channel estimation scheme with self-interference reduction for use in WPAN systems, particularly high-rate WLAN systems. The channel estimation method utilises the maximum correlation value in which self-interference caused by multipath transmission is cancelled. The estimation scheme is capable of estimating the channel distortion with little more additional hardware, with self-interference cancellation (SiC) significantly improving the performance.

**System model:** In the IEEE 802.11 standard for WLANs, the  $m$ th complex CCK code word with  $K$  chips is expressed as

$$\begin{aligned} C^m(t) &= \sum_{i=0}^{K-1} P(t - iT_c) e^{j\Phi_i^m} \\ &= e^{j\phi_1} \sum_{i=0}^{K-1} P(t - iT_c) e^{j\Psi_i^m} \\ &= e^{j\phi_1} \Psi^m(t) \end{aligned} \quad (1)$$

where  $K = 8$ ,  $P(t)$  is a square pulse from 0 to  $T_c$  seconds that takes a value of 1,  $e^{j\Phi_i^m}$  ( $m = 1, 2, \dots, 256$ ) is the complex element of the CCK code word, and the phase parameter  $\phi_1 \in \{0, \pi/2, \pi, -\pi/2\}$  according to the transmitted information bits. In eqn. 1, the CCK code words are expressed in terms of 64 complex codes  $\Psi^n(t)$  ( $n = 1, 2, \dots, 64$ ) and the phase parameter  $\phi_1$  contained in all  $K$  chips of the code word. Using eqn. 1, the transmitted signal can be expressed as

$$s(t) = \text{Re} \left[ \sqrt{P_w} C^m(t) e^{-j\omega_c t} \right] \quad 0 \leq t \leq T_w \quad (2)$$

where  $P_w$  is the signal power,  $\omega_c$  is the carrier angular frequency, and  $T_w = KT_c$  is the symbol duration.

Assuming the  $j$ th complex code word  $C^j(t)$  is transmitted, the complex baseband received signals  $d(t) = d_r(t) + jd_i(t)$  can be expressed as

$$d(t) = \frac{1}{2} \sum_{n=1}^N \sqrt{P_w} \alpha_n C^j(t - \tau_n) e^{j\theta_n} + \frac{1}{2} \mathbf{n}(t) \quad (3)$$

where  $\mathbf{n}(t)$  is a zero mean Gaussian noise process with spectral density  $N_0/2$ ,  $N$  is the number of multipath components,  $\alpha_n$ ,  $\theta_n$  and  $\tau_n$  are the amplitude, phase and delay of the  $n$ th multipath, respectively.

**Coherent detector with SiC for high-rate WPAN systems:** As shown in Fig. 1, the channel estimation method utilises the decision variable of the previous symbol in which the self-interference caused by multipath transmission is cancelled.

(i) **Self-interference cancellation block:** For the  $l$ th tracked path, the interference signal due to the remaining  $L - 1$  multipaths is reconstructed with the previous channel coefficients and the detected CCK code words of other  $L - 1$  tracked multipaths

$$r_l^m(t) = \frac{\sqrt{E_w}}{2} \sum_{\substack{n=1 \\ n \neq l}}^L \hat{c}_{n,t-1} e^{j\hat{\phi}_1} \hat{\Psi}^m(t - \tau_n) \quad (4)$$

where  $L$  is the number of tracked RAKE branches,  $\hat{c}_{n,t-1}$  is the estimated channel coefficient of the  $n$ th path in the previous symbol,  $\hat{\phi}_1$  is the estimation of the transmitted phase parameter  $\phi_1$ , and  $\hat{\Psi}^m(t)$  is the code word estimated by the maximum correlation selection block. The reconstructed replica of the self-interference,  $r_l^m(t)$ , is removed from the output of the lowpass filter  $d(t)$ , which results in  $\hat{d}(t)$ .